Physics Letters A 375 (2011) 2456–2459

Contents lists available at ScienceDirect

Physics Letters A

www.elsevier.com/locate/pla

$KAgF_3$: Quasi-one-dimensional magnetism in three-dimensional magnetic ion sublattice

Xiaoli Zhang [a], Guoren Zhang [a], Ting Jia [a], Ying Guo [a], Zhi Zeng [a,*], H.Q. Lin [b]

[a] Key Laboratory of Materials Physics, Institute of Solid State Physics, Chinese Academy of Sciences, Hefei 230031, PR China
[b] Department of Physics and Institute of Theoretical Physics, The Chinese University of Hong Kong, Shatin, Hong Kong, PR China

ARTICLE INFO

Article history:
Received 5 February 2011
Received in revised form 5 May 2011
Accepted 8 May 2011
Available online 11 May 2011
Communicated by R. Wu

ABSTRACT

The electronic structure and magnetic properties of the Jahn–Teller-distorted perovskite $KAgF_3$ have been investigated using the full-potential linearized augmented plane-wave method. It is found that $KAgF_3$ exhibits significant quasi-one-dimensional antiferromagnetism with the ratio of exchange constant $|J_\perp|$ (perpendicular to the z-axis) and J (along the z-axis) about 0.04, although the sublattice of magnetic ion is three-dimensional. The strong quasi-one-dimensional antiferromagnetism originates from the C-antiferro-distortive orbital ordering of the Ag^{2+} $4d^9$ ions. The orbital ordered antiferromagnetic insulating state in $KAgF_3$ is determined by on-site Coulomb repulsion to a large extent.

1. Introduction

Low-dimensional magnets have unique electronic and magnetic properties. For example, the physical properties of quasi-two-dimensional (2D) high-temperature superconductor [1,2], spin-Peierls compound [3], Haldane chain [4] and spin-ladder [5] as well as spin-frustrated systems [6,7] have been extensively investigated. In most of the low-dimensional magnets, the magnetic cation sublattices consist of planes or chains which are kept reasonably far apart. Materials which exhibit three-dimensional (3D) magnetic ion sublattice and low-dimensional magnetic behavior have been of interest to both experimentalist and theorists [8–12]. Up to date, the electronic orbital ordering (OO) is considered as an essential factor in determining the strong spacial exchange anisotropy in these materials.

$KAgF_3$ is a material which exhibit strong spacial exchange anisotropy within 3D magnetic Ag^{2+} ion sublattice [13]. It was first synthesized in 1971 by Odenthal et al. [14] and received, as well as other silver fluorides, attention due to the pursuit of superconductivity [15–17] in transition-metal compounds other than the cuprates. Previous experimental studies [13,17] have provided the evidence of its antiferromagnetism with $T_N = 64$ K as well as the insulating characteristic below this temperature. In contrast to the undoped cuprates that are quasi-2D antiferromagnetic (AFM) insulator, $KAgF_3$ was reported as a quasi-one-dimensional (1D) antiferromagnet using LSDA + U method [13]. However, more efforts are still needed to well understand the origin of the quasi-1D antiferromagnetism.

In the present work, we investigate the electronic structure and the magnetic properties of $KAgF_3$ using density functional theory (DFT). The calculated $J_\perp/|J| = 0.04$ confirms that the compound is a quasi-1D antiferromagnet. Here, J ($J_\perp$) refers to exchange constant along (perpendicular to) the z-axis. The quasi-1D antiferromagnetism can be understood by the C-antiferro-distortive OO which can be obtained in the presence of on-site Coulomb repulsion U. The picture of OO and AFM insulating state is thus very similar to that of an isoelectronic and isostructural compound, $KCuF_3$.

2. Calculation methods

Our electronic structure calculations are performed within the full-potential linearized augmented plane-wave framework [18]. The generalized gradient approximation (GGA) of Perdew–Burke–Ernzerhof form is adopted [19]. To include the on site Coulomb interaction GGA + U (U = on-site Coulomb repulsion strength) approach is used with $U_{\text{eff}} = U - J$ (J is the exchange interaction) instead of U [20]. Here in our work, on-site Coulomb repulsion U is applied to Ag 4d orbitals only. The Muffin-tin sphere radii are chosen to be 2.24, 2.09, and 1.85 bohr for K, Ag, and F atoms, respectively. Within the Muffin-tin sphere the electrons behave as they were in the free atom, and the wave functions are expanded using radial functions (solutions to the radial part of Schröinger equation) times spherical harmonics. Out of the Muffin-tin spheres wave functions are expanded using plane waves. The value of $R_{\text{MT}}K_{\text{max}}$ (the smallest muffin-tin radius multiplied by the maximum k value in the expansion of plane waves in the basis set) is set to 7.0. We use 500 k points (i.e., 192 k points in the irreducible wedge of the Brillouin zone) for the integration over the Brillouin zone. Self-consistency was considered to be achieved when the

* Corresponding author.
E-mail address: zzeng@theory.issp.ac.cn (Z. Zeng).

0375-9601/$ – see front matter
doi:10.1016/j.physleta.2011.05.025

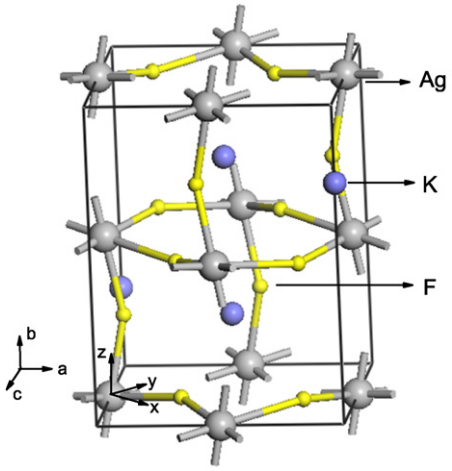

Fig. 1. Crystal structure of $KAgF_3$. The blue, gray and yellow spheres represent K, Ag and F atoms, respectively. (For interpretation of the references to color in this figure legend, the reader is referred to the web version of this Letter.)

total energy difference between succeeding iterations is less than 10^{-5} Ry/unit cell. The present setup ensures a sufficient accuracy of the calculations.

In our study, we carry out total energy calculations with three distinct spin states of (1) ferromagnetic (FM), (2) *A*-AFM (ferromagnetism in *xy* plane, AFM stacking), and (3) *G*-AFM (antiferromagnetsm in *xy* plane, AFM stacking).

3. Results and discussions

The calculations were performed for orthorhombic structure proposed by Mazej et al. [13], space group *Pnma* (No. 62), with the lattice constants $a = 6.2689$ Å, $b = 8.3015$ Å, $c = 6.1844$ Å (see Fig. 1). In our calculations we use for each AgF_6 octahedron such corresponding local *xyz* coordinates that the *z*-axis is along the *b*-axis and the *x*- and *y*-axes are approximately along the inplane nearest neighbor Ag–Ag directions. In $KAgF_3$, the Ag ion sublattice forms a pseudocubic structure, in which Ag–Ag distance along *z*-direction is slightly shorter than that in the *xy* plane. There are two types of F sites. One connects the Ag ions along the *z*-axis (named as F_{ap}) and the other connects the Ag ions in the *xy* plane (named as F_{pl}). The AgF_4 planes are slightly puckered since the F_{pl} ions have a 0.31 Å displacement from the plane formed by Ag ions. Each Ag and its six near F ions form a Jahn–Teller (JT) distorted AgF_6 octahedron. The distortion leads to the alternating long and short Ag–F bonds along the *x*- and *y*-axes. The four shorter Ag–F bonds are almost identical. The cooperative JT distortion provides a signature of an orbital ordering (OO) at the Ag^{2+} sites, which determines the electronic structure as well as the magnetic properties.

In order to clarify the electronic structure and the origin of the quasi-1D magnetism in $KAgF_3$, our calculations are designed in two stages. We start the study within GGA. To account for a possible lattice distortion, we carried out an optimization of the atomic positions, keeping the unit-cell parameters fixed and relaxing the atomic coordinates. The structural optimization shows that the Ag–F_{ap} bond is elongated by 0.012 Å and the in-plane longer (shorter) Ag–F_{pl} bond is shortened (elongated) by 0.085 Å (0.038 Å) as compared with the experimentally observed structure. As a result, the large in-plane distortion of about 0.3 Å found experimentally, decreases to 0.2 Å theoretically. Moreover, the GGA results for the optimized structure show that the FM, *A*-AFM and *G*-AFM spin states are not stable and converge to nonmagnetic (NM) metallic solution. Fig. 2 shows the total and the orbital-resolved density

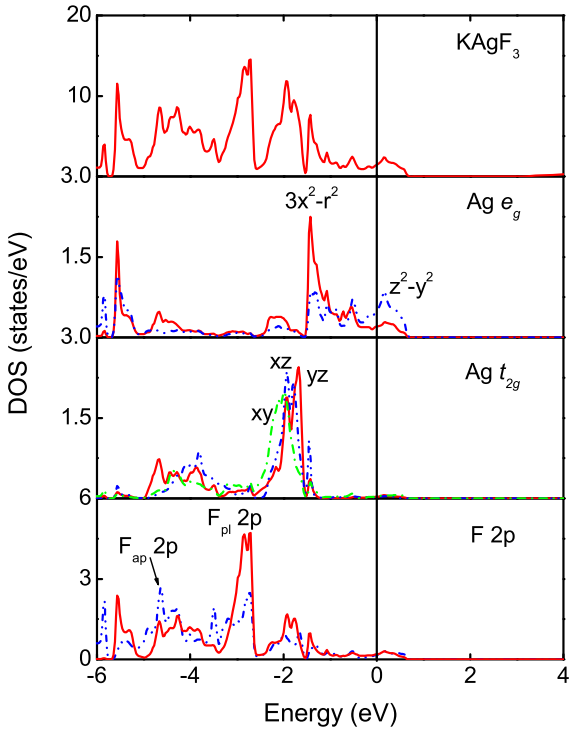

Fig. 2. (Color online.) The total and partial DOS of GGA optimized structure for nonmagnetic state obtained in GGA. The Fermi level is set at zero energy.

of states (DOS) for the NM $KAgF_3$. The distortive AgF_6 octahedron crystal field splits the Ag^{2+} $4d^9$ orbitals into fully occupied t_{2g} (xz, xy, yz) and three fourth occupied e_g $(z^2 - y^2, 3x^2 - r^2)$ orbitals. Both the anti-bonding Ag $d_{z^2-y^2}$ and $d_{3x^2-r^2}$ bands cross the Fermi level with large band widths of about 3 eV and have strong covalency [16] with the F orbitals. The band center of the $d_{z^2-x^2}$ is higher in energy than that of $d_{3y^2-r^2}$ orbital. Thus, the JT distortion generates a crystal-field splitting which is not large enough to separate the two e_g bands. Even the GGA calculations for the experimental structure still give a NM metallic solution for all the enforced spin states, in accordance with the previously published work [13]. Unlike the electronic structure of GGA optimized structure with two type of e_g bands crossing the Fermi level, the distortion alone separates the e_g bands with only one of them cross the Fermi level (not shown). Therefore, the GGA calculations cannot reproduce the insulating AFM nature of $KAgF_3$. This is in contrast to another fuoroargentate Cs_2AgF_4 in which JT distortion alone can lead to the orbital ordered insulating state [21–23].

As the second stage, we concern the correlation interaction by GGA + *U* approach. In general, strong on-site Coulomb repulsion *U* increases the localization of *d* electrons and favors orbital ordering and/or magnetic order. However, the magnitude of the correlation for the Ag^{2+} ion is not known. In order to determine its value, we performed a structural optimization as a function of *U* (1–6 eV) and found the *U* value with which the equilibrium structure matches the experimental one. This scheme to extract the Coulomb parameter is feasible because the on-site Coulomb repulsion *U* determines the orbital polarization of the e_g states for a large extent, which, in turn, causes the structural JT lattice distortion. The optimized inequivalent Ag–F distances d_1, d_2 and d_3 are shown in Fig. 3. We find that the optimized structure for $U = 5.0$ eV is the closest to the one obtained experimentally. And thus this *U* is adopted as the most reliable one. This value is smaller than the commonly used $U = 7$–9 eV value for Cu^{2+} but still reasonable, because the 4*d* orbitals of an Ag^{2+} ion are less contracted than the 3*d* orbitals of a Cu^{2+} ion.

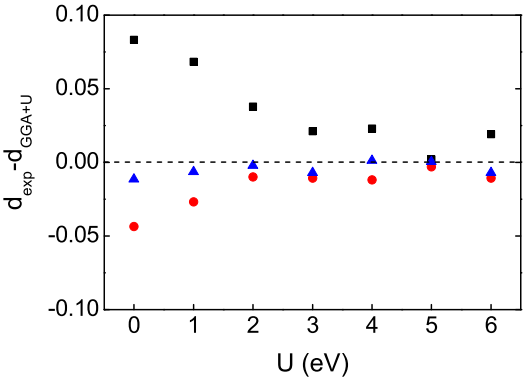

Fig. 3. (Color online.) Deviation of relaxed inequivalent Ag–F distances d_1, d_2 and d_3 from the experiment as a function of the Coulomb repulsion U. The data of $U = 0$ denotes the GGA optimized results.

Table 1
Electronic structure of $KAgF_3$ in FM, A-AFM and G-AFM spin states obtained by GGA + U with $U = 5$ eV. The total energy difference (ΔE, meV/4f.u.), the energy gap (E_g, eV), the local spin moment (SM, μ_B) of each Ag, apical F (F_{ap}), and planar F (F_{pl}) atoms are shown.

	ΔE	E_g	Ag-SM	F_{ap}-SM	F_{pl}-SM
FM	272	0.5	0.67	0.12	0.1
A-AFM	0	1.5	±0.62	0	±0.09
G-AFM	23	1.4	±0.6	0	±0.09

The GGA + U (5 eV) total energy calculations of various spin states shown in Table 1 indicate that the ground spin state is the A-AFM insulating state. The obtained ground spin state is in accordance with the previous LSDA + U results [13]. This indicates that the on-site Coulomb repulsion is important in determining the AFM insulating properties in $KAgF_3$. We note that the difference in total energy between the A-AFM and G-AFM spin states is as small as 23 meV/4f.u., while the energy difference between the A-AFM and FM spin states is about 272 meV/4f.u. We should notice the fact that A-AFM and G-AFM spin states have opposite ordering in the xy plane but the same ordering along the z direction, whereas both the A-AFM and FM spin states have the same ordering in the xy plane but different ordering along the z-axis. This reveals that AFM exchange interactions along the z direction are more favorable and robust than FM coupling in the xy plane, indicating a strong spacial exchange anisotropy in $KAgF_3$.

To gain additional insight into the spacial exchange anisotropy, we evaluate the magnetic exchange constants along and perpendicular to the z-axis numerically in terms of the Heisenberg spin Hamiltonian:

$$H = J \sum_{i,j} \mathbf{S}_i \cdot \mathbf{S}_j + J_\perp \sum_{k,l} \mathbf{S}_k \cdot \mathbf{S}_l \tag{1}$$

where the first (second) term refers to summing over all nearest neighbors along (perpendicular to) the z-axis. By mapping the obtained total energies for each magnetic state to the next nearest Heisenberg model, the exchange interactions J and $J_\perp$ are

$$J = \frac{1}{8S^2}(E_{\text{FM}} - E_{A\text{-AFM}}) \tag{2}$$

$$J_\perp = \frac{1}{16S^2}(E_{A\text{-AFM}} - E_{G\text{-AFM}}) \tag{3}$$

With the spin $S = 1/2$ of a $4d^9$ Ag^{2+} ion, we get $J = 136$ meV and $J_\perp = -5.8$ meV, indicating strong AFM coupling along the z-axis and a much weaker FM coupling in the xy plane. $|J_\perp|/J = 0.04$ reflects strong quasi-1D magnetism in $KAgF_3$. Thus, it has been concluded that $KAgF_3$ is another material exhibiting quasi-1D magnetic behavior within 3D magnetic ions sublattice, which is in accordance with the results of Mazej et al. [13]. The relatively large J and $J_\perp$ values are consistent with the findings that the DFT electronic structure calculations generally overestimate the magnitude of spin exchange interactions [24].

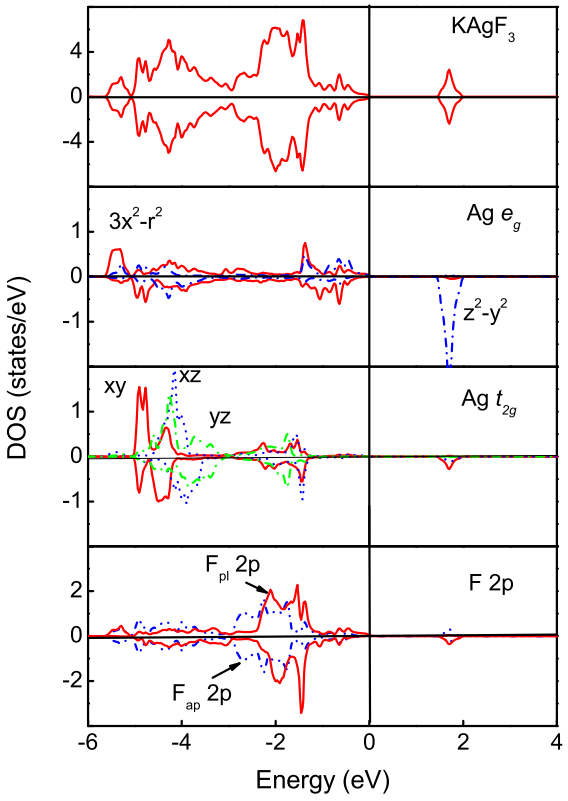

Fig. 4. (Color online.) The total and partial DOS of $KAgF_3$ for A-AFM spin state from GGA + U with $U = 5$ eV. The up and down panels in each DOS plot denote the spin-up and spin-down states respectively.

The quasi-1D magnetic behavior can be understood from the ground state electronic structure and OO of $KAgF_3$. The total and the orbital-resolved DOS for the A-AFM spin state experimental structure are shown in Fig. 4. The Coulomb repulsion U pushes the occupied and unoccupied $4d$ levels downward and upward respectively and opens up an insulating gap. It is obvious that the one hole states mainly occupy the higher level $d_{z^2-y^2}$ bands and the orbital polarization of e_g states is enhanced. Actually, due to the strong Ag–F covalency [16] the one hole spreads over the six fluorine atoms of the AgF_6 octahedron. This is also reflected by the magnitude of local spin magnetic moments within each muffin-tin sphere, ±0.62 μ_B/Ag, 0μ_B/F_{ap} and ±0.09 μ_B/F_{pl} (see Table 1). The hole states have alternating $d_{z^2-y^2}$ and $d_{z^2-x^2}$ symmetry for Ag^{2+} ions in the xy plane (see the last panel in Fig. 5) because of the cooperative JT distortion. The in-plane $d_{z^2-x^2}/d_{z^2-y^2}$ OO repeats along the z-axis and C-antiferro-distortive OO is formed, which is clearly shown in Fig. 5. The overlap of Ag–F–Ag along the z-axis (see the upper and middle panel in Fig. 5) is larger than that in the xy plane (the lower panel in Fig. 5) leading to the dominate magnetic interaction along z-axis. The C-antiferro-distortive OO would immediately give A-AFM spin state, according to Goodenough–Kanamori–Anderson rules. Also, our GGA + U calculation results confirm this mechanism since it shows that the A-AFM state is indeed more stable than the G-AFM and FM states (see Table 1). Therefore, the results of our calculations have clearly

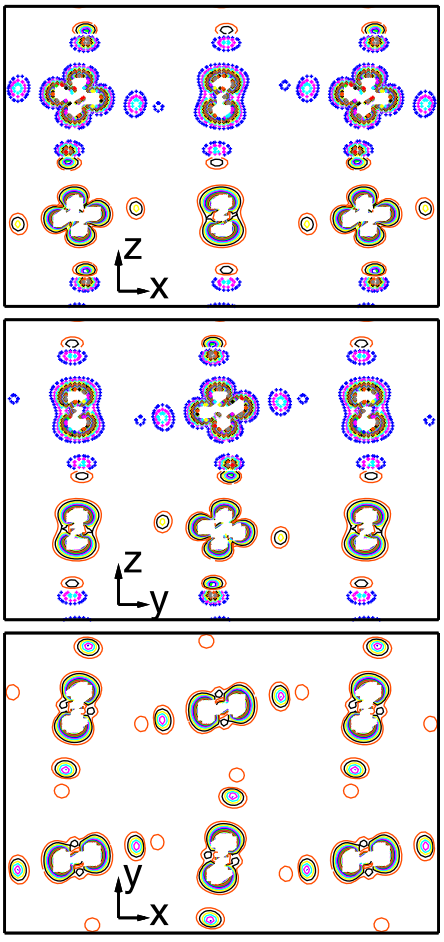

Fig. 5. (Color online.) The contour plot of spin density in *xz* (upper panel), *yz* (middle panel) and *xy* (lower panel) planes of $KAgF_3$ for *A*-AFM state from GGA + *U* (5 eV). The solid (dot) lines depict the spin-up (spin-down) states.

illustrated that $KAgF_3$ is an orbitally ordered quasi-1D AFM insulator, in close analogy to $KCuF_3$.

4. Conclusions

By GGA and GGA + *U* electronic structure calculations, we have found the quasi-one-dimensional (1D) antiferromagnetism of $KAgF_3$ with $J_\perp/|J| = 0.04$, which may stimulate further experimental studies. Here, J ($J_\perp$) refers to exchange constant along (perpendicular to) the *z*-axis. The quasi-1D antiferromagnetism can be understood by the *C*-antiferro-distortive orbital ordering. The orbital ordered insulating state can only be obtained when the on-site Coulomb repulsion of Ag 4*d* electrons is in consideration. With $U = 5$ eV for Ag 4*d* electrons the optimized structure is in the best agreement with experiment. The picture of orbital ordering and AFM insulating state is thus very similar to that of an isoelectronic and isostructural compound, $KCuF_3$.

Acknowledgements

This work was supported by the special Funds for Major State Basic Research Project of China (973) under Grant No. 2007CB925004, Knowledge Innovation Program of Chinese Academy of Sciences under Grant No. KJCX2-YW-W07, Director Grants of CASHIPS, and CUHK Direct Grant No. 2160345. Part of the calculations were performed in Center for Computational Science of CASHIPS.

References

[1] G. Shirane, Y. Endoh, R. Birgeneau, M. Kastner, Y. Hidaka, M. Oda, M. Suzuki, T. Murakami, Phys. Rev. Lett. 59 (1987) 1613.
[2] Y. Kamihara, T. Watanabe, M. Hirano, H. Hosono, J. Am. Chem. Soc. 130 (2008) 3296.
[3] M. Shaz, S. van Smaalen, L. Palatinus, M. Hoinkis, M. Klemm, S. Horn, R. Claessen, Phys. Rev. B 71 (2005) 100405(R).
[4] H. Tsunetsugu, Y. Motome, Phys. Rev. B 68 (2003) 060405(R).
[5] O. Pieper, B. Lake, A. Daoud-Aladine, M. Reehuis, K. Prokes, B. Klemke, K. Kiefer, J.Q. Yan, A. Niazi, D.C. Johnston, A. Honecker, Phys. Rev. B 79 (2009) 180409(R).
[6] H. Kageyama, K. Yoshimura, K. Kosuge, H. Mitamura, T. Goto, J. Phys. Soc. Jpn. 66 (1997) 1607.
[7] S.K. Pandey, Maiti Kalobaran, Phys. Rev. B 78 (2008) 045120.
[8] J. Tong, C. Lee, M.-H. Whangbo, R.K. Kremer, A. Simon, J. Koehler, Solid State Sciences 12 (2010) 680.
[9] S.K. Satija, J.D. Axe, G. Shirane, H. Yoshizawa, K. Hirakawa, Phys. Rev. B 21 (1980) 2001.
[10] G. Giovannetti, S. Margadonna, J. van den Brink, Phys. Rev. B 77 (2008) 075113.
[11] Y. Xiao, Y. Su, H.-F. Li, C.M.N. Kumar, R. Mittal, J. Persson, A. Senyshyn, K. Gross, Th. Brueckel, Phys. Rev. B 82 (2010) 094437.
[12] M.D. Towler, R. Dovesi, V.R. Saunders, Phys. Rev. B 52 (1995) 10150.
[13] Z. Mazej, E. Goreshnik, Z. Jagličić, B. Gaweł, W. Łasocha, D. Grzybowska, T. Jaroń, D. Kurzydłowski, P. Malinowski, W. Koźminski, J. Szydłowska, P. Leszczyński, W. Grochala, Cryst. Eng. Comm. 11 (2009) 1702.
[14] R.H. Odenthal, R. Hoppe, Monatsh. Chem. 102 (1971) 1340.
[15] W. Grochala, R. Hoffmann, Angew. Chem., Int. Ed. 40 (2001) 2742.
[16] W. Grochala, R.G. Egdell, P.P. Edwards, Z. Mazej, B. Žemva, Chem. Phys. Chem. 4 (2003) 997.
[17] W. Grochala, P.P. Edwards, Phys. Status Solidi B 240 (2003) R11.
[18] P. Blaha, K. Schwarz, G. Madsen, D. Kvasnicka, J. Luitz, http://www.wien2k.at.
[19] J.P. Perdew, K. Burke, M. Ernzerhof, Phys. Rev. Lett. 77 (1996) 3865.
[20] V.I. Anisimov, I.V. Solovyev, M.A. Korotin, M.T. Czyzyk, G.A. Sawatzky, Phys. Rev. B 48 (1993) 16929.
[21] H. Wu, D.I. Khomskii, Phys. Rev. B 76 (2007) 155115.
[22] D. Kasinathan, K. Koepernik, U. Nitzsche, H. Rosner, Phys. Rev. Lett. 99 (2007) 247210.
[23] X. Hao, Y. Xu, Z. Wu, D. Zhou, X. Liu, J. Meng, Phys. Rev. B 76 (2007) 054426.
[24] D. Dai, M.-H. Whangbo, J. Chem. Phys. 114 (2001) 2887.